ELSEVIER

PII: S0032-3861(97)10146-X

Polymer Vol. 39 No. 20, pp. 4801–4816, 1998

0032-3861/98/$19.00+0.00

Studies on comonomer compositional distribution of the bacterial poly(3-hydroxybutyric acid-co-3-hydroxypropionic acid)s and crystal and thermal characteristics of their fractionated component copolyesters

Amin Cao[a], Ken-ichi Kasuya[b], Hideki Abe[b], Yoshiharu Doi[b] and Yoshio Inoue[a,*]
[a]*Department of Biomolecular Engineering, Tokyo Institute of Technology, 4259 Nagatsuta, Midori-ku, Yokohama 226, Japan*
[b]*The Institute of Physical and Chemical Research (RIKEN), 2-1 Hirosawa, Wako-city, Saitama 351-01, Japan*
(Received 1 August 1997; revised 11 September 1997; accepted 29 September 1997)

Two different kinds of natural poly(3-hydroxybutyric acid-co-3-hydroxypropionic acid)s [P(3HB-co-3HP)] with individual 3HP comonomer contents of 36.5 and 68.1 mol.% were biosynthesized by the bacteria *Alcaligenes latus*, fed on the cosubstrates of (*R*)-3-hydroxybutyric acid (3HBA) and 3-hydroxypropionic acid (3HPA). Employing the mixed chloroform/*n*-heptane solvent, the bacterial products were found to be fractionated into a number of fractions, and the presence of broad comonomer compositional distributions was unambiguously demonstrated. A deep insight into fractionation provided by means of g.p.c. and n.m.r. spectrometry confirmed that the fractionations were predominantly governed by the factor of comonomer composition, while the effect of molecular weight was not so significant. ^{13}C n.m.r. investigation of carbonyl diad sequence distributions for the fractionated copolyesters along with the original bacterial product clearly revealed that the copolymerization occurring in the bacterial cell bodies was virtually in accordance with the random copolymerization model, and this feature was, however, obscured due to the presence of comonomer compositional distribution. Further, the crystal structures and thermal behaviors were investigated via WAXD and d.s.c. for the fractionated copolyesters with 3HP comonomer content spanning the whole comonomer composition. These investigations showed that both 3HB- and 3HP-rich copolyesters formed different 2_1 helix crystal structures, respectively, corresponding to the P(3HB) and P(3HP) types of lattice structures with distinctive fiber repeats, while those bearing intermediate 3HP content (about 48–75 mol.%) appeared as the amorphous state. The existence of the minor comonomer drastically retarded the crystallizability of either 3HB- or 3HP-rich copolyester chains; however, the glass transition behaviors reflected that the chain mobility in the amorphous state was enhanced linearly with the increase in the 3HP unit content. Moreover, the growth rates and morphologies of spherulites for the fractionated copolyesters revealed that the growth rates were markedly suppressed by the incorporated minor comonomer, and the uncrystallizable chains were likely trapped in the interfibrillar regions.

(Keywords: P(3HB-co-3HP); copolyester; comonomer compositional distribution)

INTRODUCTION

A variety of poly(hydroxyalkanoic acids) [PHAs] can be accumulated in various kinds of bacteria in nature[1–4]. These aliphatic polyesters are now of increasing interest to both researchers and industrialists because of their favoring properties of biodegradability and biocompatibility[1–3]. Recently, it has been reported that a lot of copoly(hydroxyalkanoic acids) can be efficiently synthesized by several kinds of bacteria. The variability in either the carbon number of repeating unit or pendant chain will lead to the variation of physical and biodegradable features of bacterially synthesized PHAs, e.g., incorporating second monomer units such as 3-hydroxyvaleric acid (3HV)[5,6], 3-hydroxypropionic acid (3HP)[7–13], 4-hydroxybutyric acid (4HB)[14–16], 3-hydroxyhexanoic acid (3HH)[17,18], and so forth, into the chains of poly(3-hydroxybutyric acid) (P(3HB)), can produce a great number of copolyesters with desirable properties. Since the 3HP unit does not bear the side chain at the β-site, its segmental mobility can, therefore, be reasonably expected to be relatively higher than that of the 3HB unit. Yamashita *et al.*[19] have reported that poly(β-propiolactone) (P(3HP)) exhibits a large elongation rate up to 540%. Hence, the incorporation of the 3HP unit into P(3HB) can be expected to improve the disadvantageous features for P(3HB), such as excessive brittleness and high melting point[1–3].

In general, it is also well-known that comonomer composition as well as comonomer compositional distribution are also important factors regulating the melting point, crystallite morphology and aggregating state of copolymer. Mitomo *et al.*[21] have reported that bacterial copolyester P(3HB-co-3HV) could be fractionated into fractions with different comonomer composition by a water/acetone mixed solvent system. Employing the mixed solvent system of chloroform and *n*-heptane, the comonomer compositional

* To whom correspondence should be addressed

distribution of commercially available bacterially synthesized P(3HB-co-3HV) samples have also been investigated by Yoshie *et al.*[22], and broad and complex features of comonomer compositional distributions have been unambiguously revealed. Practically, there are two conventional fractionating techniques for analyzing the comonomer compositional distribution of a copolymer, including solvent/nonsolvent and temperature-raising elution fractionation (TREF) methods[23,24], and the latter is especially useful for semicrystalline copolymer with composition-dependent crystallizability. In principle, the phase segregation occurring in the polymer solution is governed by the Gibbs free energy of mixing (ΔF_m),

$$\Delta F_m = \Delta H_m - T\Delta S_m \quad (1)$$

where ΔH_m and ΔS_m are the mixing enthalpy and entropy, respectively. Further, according to Hildebrand–Scott solubility parameter theory[25], the mixing enthalpy (ΔH_m) can be expressed as

$$\Delta H_m = V\phi_1\phi_2(\delta_1 - \delta_2)^2 \quad (2)$$

where ϕ_1 and ϕ_2 are the volumetric fractions of polymer and solvent, δ_1 and δ_2 are their corresponding solubility parameters, and V is the total volume of polymer solution. In the case of mixed solvent, δ_2 can be rewritten as

$$\delta_2 = \delta_{s1}\phi_{s1} + \delta_{s2}\phi_{s2} \quad (3)$$

in which ϕ_{s1} and ϕ_{s2} are the volume fractions of two kinds of solvents (s_1 and s_2) in the mixed solvent, δ_{s1} and δ_{s2} are their individual solubility parameters. Varying the values of ϕ_{s1} and ϕ_{s2}, ΔF_m can consequently be optimized to suitable values under a given operating temperature. Hence, for an investigated copolymer, the components with different comonomer compositions are practically fractionated owing to their distinctive δ_2 at the precipitating point.

In the previous work[13], bacterially synthesized P(3HB-co-3HP) bearing 30.6 mol.% 3HP comonomer unit has been fractionated by the mixed solvent chloroform/*n*-heptane, and a broad comonomer compositional distribution was indeed revealed. Further, the dependence of thermal and crystallization behaviors on 3HP comonomer composition of the fractionated samples were thereby demonstrated.

In this presentation, utilizing the mixed carbon sources of (*R*)-3-hydroxybutyric acid (3HBA) and 3-hydroxypropionic acid (3HPA), we biosynthesized two kinds of P(3HB-co-3HP)s with the average 3HP comonomer fractions of 36.5 and 68.1 mol.% by the bacteria *Alcaligenes latus*. Subsequently, these two 'original' copolyesters were fractionated via the chloroform/*n*-heptane mixed solvent system. The effects of comonomer composition and molecular weight on the fractionating procedure are carefully investigated by means of g.p.c. and n.m.r. spectrometry. Inspecting the wide-angle X-ray diffraction patterns, crystal structures of either 3HB- or 3HP-rich samples are critically discussed. Moreover. the thermal and crystallization behaviors will be characterized for the fractions with narrower comonomer compositional distribution.

EXPERIMENTAL SECTION

Materials

Bacterial homopolyester P(3HB), purchased from Aldrich Chem. Inc. (Lot no. 00925KF), was used after purification with chloroform and *n*-hexane. Poly(β-propiolactone) [P(3HP)], chemically synthesized through ring-opening polymerization, was supplied by Tokuyama Co. (Tsukuba, Japan), which was also purified in the same way as used for P(3HB). Two kinds of P(3HB-co-3HP)s with 3HP content of 36.5 and 68.1 mol.% were biosynthesized by the bacteria *Alcaligenes latus* (ATTC 29713) fed on the mixed carbon substrates of (*R*)-3-hydroxybutyric acid [(*R*)-3HBA] and 3-hydroxypropionic acid [3HPA]. The biosynthetic procedures in detail were described elsewhere[10–13], and the resultant products are summarized in *Table 1*.

The procedure of fractionation of the as-produced copolyester was as follows: the original biosynthetic product bearing an average 3HP monomer fraction of 68.1 mol.% (denoted as sample BioB0) was fractionated, utilizing the procedure as reported in our previous work[13], i.e. *n*-heptane was carefully added into the copolyester/chloroform solution (starting polymer concentration 3 g/300 ml) by an aliquot of 10 ml under gentle agitation at the ambient temperature. If the precipitated mass was firstly observed visually in the mixed solvent, the fractionated copolyester fractions were then sampled as the new precipitation occurred during another addition of 10 ml *n*-heptane, and isolated by centrifugation (8000 rpm). This procedure was repeated until adding any amount of heptane could not cause appreciable precipitation. In this study, another product bearing an average 3HP monomer fraction of 36.5 mol.% (denoted as sample BioA0) was fractionated via a modified sampling method, i.e., the precipitated copolyesters were sampled by a constant $\Delta C = 1.5$ vol.% of *n*-heptane in which ΔC means the incremental volumetric content of heptane in the mixed solvent between two continuous sampling runs.

Analytical procedures

Molecular weights of polyester samples were measured by a Toso HLC-8020 Gel Permeation Chromatography (g.p.c.) instrument equipped with a Toso-8010 controller and a refractive detector. Chloroform was used as the eluant at a flowing rate of 1.0 ml/min. Polystyrenes with low polydispersity were employed as the standards to generate the calibration curve, then M_n, M_w and polydispersity index (PDI = M_w/M_n) were calculated through a SC-8010 data processor.

Measurements of ^{1}H n.m.r. spectra were performed in $CDCl_3$ solution on a JEOL GSX-270 spectrometer operating in PFT mode at 270 MHz and 25°C. ^{1}H n.m.r. spectra were recorded with 4.5 μs pulse width (45° pulse), 5 s pulse repetition time, 4000 Hz spectral width, 32 K data points and 32 FID accumulations. 3HP mole fractions of the fractionated samples along with original products were estimated from the relative intensities of $CH_2(7)$ and CH(3) resonances as illustrated in *Figure 1*[11–13]. ^{13}C n.m.r. spectra were measured in $CDCl_3$ solution at 67.8 MHz and 25°C with a 8.2 μs pulse width (90° pulse), 27 027 Hz spectral width, 64 K data points, 5 s pulse repetition time and 16 000–20 000 FID accumulations.

Wide-angle X-ray diffraction (WAXD) patterns were recorded on Rigaku RU-200 (50 kV/180 mA) and Rigaku IP R-AXIS-DS3 systems. The nickel-filtered Cu Kα X-ray beams with a pinhole graphite monochrometer (λ = 0.15418 nm) were used as the source. WAXD patterns were measured in a 2θ range of 6–40° at a scanning speed of 1°/min. Samples for WAXD measurements prepared by solvent casting technique were allowed to isothermally crystallize at room temperature for more than 4 weeks prior to analysis. The degrees of crystallinity were estimated according to the method developed by Vonk[26].

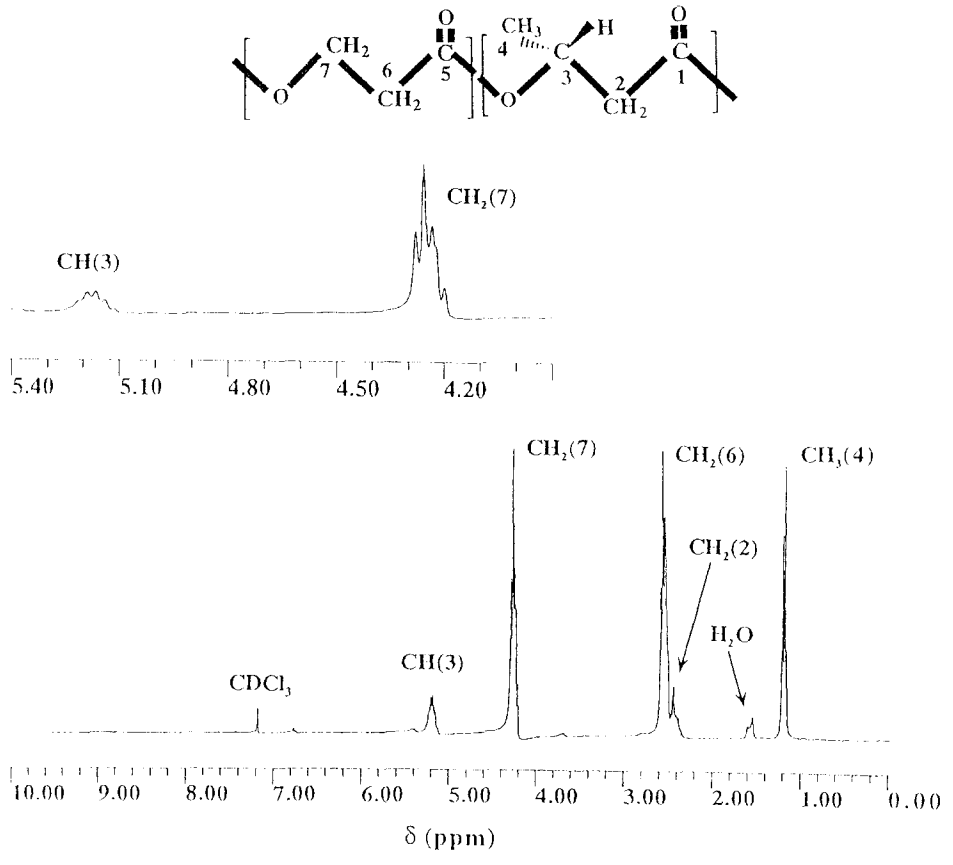

Figure 1 The 270 MHz ^{1}H n.m.r. spectrum of the fractionated P(3HB-co-3HP) (fraction AF1) with 73.6 mol.% 3HP unit in $CDCl_3$ solution

Table 1 Preparation of P(3HB-co-3HP)s from *R*-(−)-3-hydroxybutyric acid (3HBA) and 3-hydroxypropionic acid (3HPA) by *Alcaligenes latus*[a]

Sample code	Carbon source		Dry cell yield (g/l)	Polyester[b]				
	3HBA (g/l)	3HPA (g/l)		Yield (g/l)	Polymer (content wt.%)	3HP[c] (content mol.%)	M_n^d ($\times 10^{-5}$)	PDI[d] (M_w/M_n)
BioA0	5.0	1.0	2.51	0.64	25.5	36.5	2.65	2.53
BioB0	2.0	4.0	0.91	0.21	23.1	68.1	2.16	1.67

[a]Cultivated at 30°C and pH 7.0 for 6 days
[b]Extracted by boiling chloroform
[c]3HP monomer content was determined by ^{1}H n.m.r. in $CDCl_3$ solution
[d]M_n and PDI (M_w/M_n) were characterized by g.p.c.

Thermal analyses were performed on a Seiko Differential Scanning Calorimeter (DSC-220) equipped with a SSS5300 workstation. D.s.c. samples (2–4 mg) prepared via solvent-casting technique were pre-sealed in aluminum pans, then firstly heated to 195°C and kept for 2 min to erase their thermal histories. Subsequently, the samples were allowed to be slowly cooled to the ambient temperature and maintained for more than 4 weeks to prompt the crystallization to an equilibrium state. D.s.c. thermal diagrams were recorded in a temperature range of −80–195°C at a heating rate of 10°C/min (first heating scan). After rapidly quenching, the samples were reheated from −100 to 195°C at a heating rate of 20°C/min (second heating scan). Melting points (T_m) were taken as the peak tops of endothermic curves, and values of heat of fusion (ΔH) were calculated from the integral of endothermic curves. Glass transition temperatures (T_g) were estimated as the midpoints of heat capacity changes in the thermal diagrams measured by the second heating scan.

Measurements of isothermal spherulitic growth rates (G) were carried out on a polarized microscope, Olympus BX90, equipped with a Mettler FP82HT hot stage under designated isothermal crystallization temperatures (T_c). A piece of film (2 mg) was inserted between the glass slide and the cover glass, then heated to 195°C and kept for 2 min, in turn quickly cooled to the desired T_c and maintained. Microscopic images were monitored through a Sony CCD video camera attached to the microscope, and the real dimensions of spherulites could, therefore, be calibrated by a micrometric reticule. Rates of isothermal spherulitic growth (G) were estimated from dR/dt in which R was the radius of spherulite at a given time t.

RESULTS AND DISCUSSION

Biosyntheses and fractionation of P(3HB-co-3HP)s

Table 1 shows the results of fermentation by the bacteria *A. latus*. In this work, (*R*)-3-hydroxybutyric acid (3HBA) and 3-hydroxypropionic acid (3HPA) were utilized as the mixed carbon sources for the objective of accumulating copolyesters with higher 3HP monomer content. Varying the feeding weight ratio of 3HBA to 3HPA from 2:4 to 1:5

Table 2 Fractionation results of sample BioB0 with 68.07 mol.% 3HP

Sample code	*n*-Heptane (v/v, %)[a]	Weight (fraction, %)[b]	3HP (mol.%)[c]	M_n^d ($\times 10^{-5}$)	PDI[d] (M_w/M_n)
BioB0	—	100	68.1	2.16	2.86
BF1	31.8	8.8	95.9	2.50	1.76
BF2	33.3	8.5	89.6	1.83	2.22
BF3	34.8	10.1	86.2	2.45	1.45
BF4	36.2	11.5	77.9	1.87	3.08
BF5	37.5	8.8	75.2	2.41	1.79
BF6	38.8	9.5	68.7	2.14	2.95
BF7	40.0	9.9	65.0	1.87	1.73
BF8	41.2	8.7	56.6	1.78	2.15
BF9	43.4	16.0	53.4	2.11	3.67
BF10	46.4	4.6	48.9	1.63	3.99
BF11	48.3	2.5	31.4	0.59	2.45
BF12	50.8	1.3	42.5	n.d[e]	n.d[e]

[a]The volume ratio of *n*-heptane in the chloroform/*n*-heptane mixed solvent
[b]The weight fractions were estimated on the hypotheses that weight percentage of fractions were calculated from their amounts divided by the total yield, respectively, in which the inevitable losses were not taken into consideration
[c]3HP mole fractions were determined via ^{1}H n.m.r. ($CDCl_3$)
[d]M_n and PDI were characterized by g.p.c.
[e]Not determined

resulted in a marked increase of 3HP monomer content from 36.5 to 68.1 mol.% in the extracted copolyesters, however, either the yield of dry cells or copolyester content were drastically lowered. Considering the metabolic pathways of 3HBA and 3HPA in the cells of bacteria *A. latus* suggested by Doi *et al.*[8], 3HPA can be directly converted into 3-hydroxypropionyl-CoA, exhibiting a distinctive metabolizing feature in comparison with 3HBA. Thus, the biosynthetic processes were subjected to the individual enzymes catalyzing the respective metabolisms of 3HBA and 3HPA; consequently, the comonomer composition was regulated. Viewing the results of our foregoing[13] and present works, a good reproducibility of biosyntheses by bacteria *A. latus* is unambiguously demonstrated. Furthermore, the average number molecular weight (M_n) and yield of BioB0 (68.1 mol.% 3HP) are appreciably lower than the values of BioA0 (36.5 mol.% 3HP), reasonably indicating the relatively lower activity of synthase for 3-hydroxypropionyl-CoA in the cell bodies.

For the sake of investigating comonomer compositional distribution of the harvested copolyester P(3HB-co-3HP)s, 'original' as-produced copolyester BioB0 was fractionated by the chloroform and *n*-heptane solvent/nonsolvent method as elaborated in the previous study[13]. Results of fractionation are tabulated in *Table 2*, indicating that the lower *n*-heptane volumetric content in the mixed solvent at which the fraction was sampled, the higher 3HP monomer composition was observed. For P(3HB-co-3HV)s, Yoshie *et al.*[22] have qualitatively interpreted that the fractionation by the difference in the 3HV unit composition was originated from the distinctive polarities of pendant chains at the β site. On the basis of phase segregation theory, an attempt to clarify the fractionating phenomenon is implemented with the aid of term defined as solubility parameter δ. Empirically, the values of δ of polymers can be approximately evaluated from $\rho \times \Sigma G/M_u$[27-29] in which ΣG represents the sum of molar-attraction constants for all the atoms and groupings in the repeating unit, M_u and ρ are the molar weight of repeating unit and density of polymer. In the case of a semicrystalline polymer, ρ can be expressed as,

$$\rho = \rho_a(1 - \chi_c) + \rho_c\chi_c \quad (4)$$

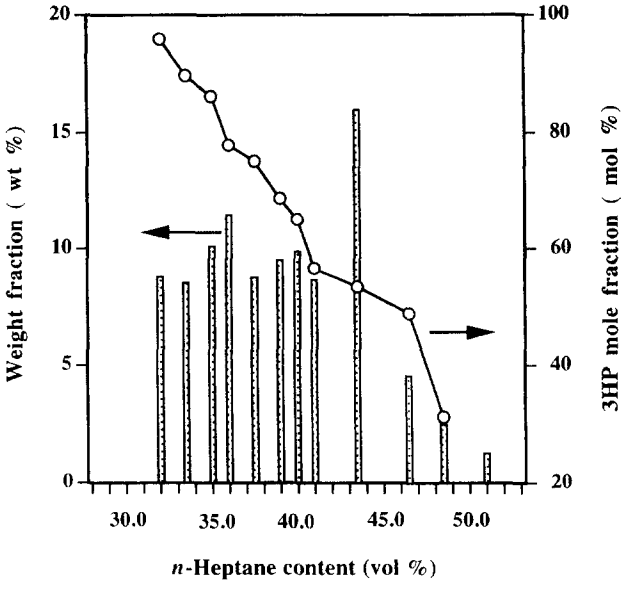

Figure 2 The weight percentage and 3HP unit content *versus* sampling *n*-heptane contents for the fractionated copolyesters originating from BioB0 (68.1 mol.% 3HP)

where ρ_a and ρ_c are the respective densities of polymer in the amorphous and crystalline states, χ_c means the degree of crystallinity. Here, δ_1 values for P(3HB) and P(3HP) were approximately calculated to be 9.8 and 11.3 $(cal/cm^3)^{1/2}$, respectively, referring to the reported data (for P(3HB), ΣG = 692.4 $(cal/cm^3)^{1/2}$ mol^{-1}, ρ_a = 1.16 g cm^{-3}, ρ_c = 1.25 g cm^{-3}, χ_c = 70%; for P(3HP), ΣG = 589.6 $(cal/cm^3)^{1/2}$ mol^{-1}, ρ = 1.38 g cm^{-3})[20,27,29,30], comparatively, the δ_2 values for chloroform and *n*-heptane[28] are 9.3 and 7.4 $(cal/cm^3)^{1/2}$. Thus, the δ_2 of the mixed solvent will be proportionally decreased with the addition of heptane, resulting in the deviation from the δ_1 value of polymer. As a result, the Gibbs free energy of mixing, ΔF_m gradually increases, and consequently the segregation of polymer chain in the mixed solvent will occur. The δ_1 values of copolyester P(3HB-co-3HP)s are expected to increase with 3HP mole fractions, hence component copolyesters bearing

higher 3HP monomer fractions can be predicted to firstly precipitate in the mixed solvent due to corresponding higher values of δ_2 (lower *n*-heptane content) at the precipitating point. This prediction is well consistent with the experimental evidence shown here and in the former paper[13]. In order to exhibit clearly the fractionating result, the dependence of both weight percentage (wt.%) and 3HP monomer content on the sampling *n*-heptane volumetric composition (vol.%) is depicted in *Figure 2*. It is seen that the resultant fractions have 3HP monomer compositions spreading from 95.9 mol.% (BF1) to 31.4 mol.% (BF11), demonstrating a broad comonomer compositional distribution. Interestingly, the fraction bearing 68.7 mol.% 3HP (BF6) is not the major component, although its comonomer composition is closest to that of the 'original' product BioB0 (68.1 mol.% 3HP). Moreover, the 3HP mole contents of fractions and the sampling *n*-heptane compositions (vol.%) show an approximately linear relation. Further, if the sampling method is taken into careful consideration, it is evident that adding 10 ml of *n*-heptane into the mixed solvent will cause an increase in *n*-heptane content. However, the rate of increase in *n*-heptane content (ΔC) will decrease in the order of sampling times owing to the increasing overall volume of mixed solvent. Recognizing that solubility parameters δ_2 are inversely proportional to the content of *n*-heptane in the mixed solvent, the fractionation procedure, that is, adding 10 ml of *n*-heptane every time, probably causes the heterogeneous origin of fractionation which likely obscures the 'true' feature of comonomer compositional distribution. For example, apparently, the sample of fraction BF9 has the largest weight percentage, but that may be virtually originated from the excessive addition of *n*-heptane (20 ml) or an enlarged ΔC.

In order to reveal the 'true' behavior of comonomer compositional distribution behaviors for the biosynthesized copolyesters as possible, the 'original' copolyester BioA0 with 36.5 mol.% 3HP was fractionated by the modified fractionating method, i.e., ΔC was designated to be 1.5 vol.%, a fixed variation of *n*-heptane volumetric content in the mixed solvent for each sampling time. Result of fractionation is depicted in *Figure 3*, indicating an approximately linear relationship between 3HP mol.% of fractions and sampling *n*-heptane content. The deviation from the linearity for AF6 (21.9 mol.% 3HP) having the largest weight percentage can be rationalized by the conventional phenomenon known as interchain entanglement which most probably occurs in the case of large amount of precipitation. In addition, the relationship between 3HP mol.% of fractions and their corresponding sampling *n*-heptane content (vol.%) is hereby plotted in

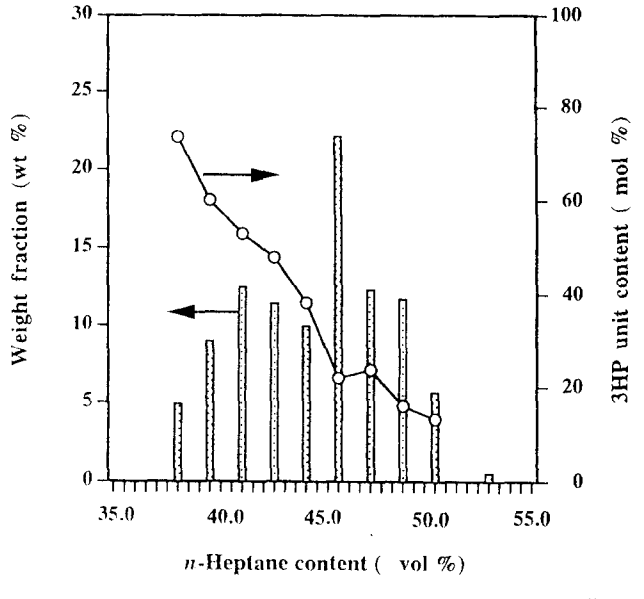

Figure 3 The weight percentage and 3HP unit content *versus* sampling *n*-heptane contents for the fractionated copolyesters originating from BioA0 (36.5 mol.% 3HP)

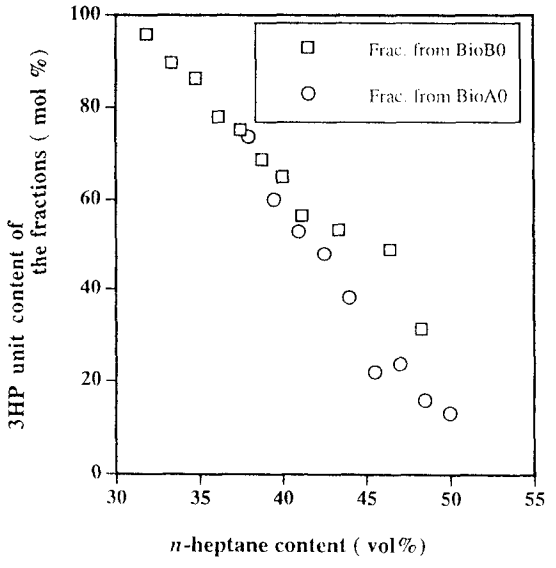

Figure 4 The 3HP unit content *versus* sampling *n*-heptane content in the mixed solvent for the fractions originating from both BioA0 and BioB0

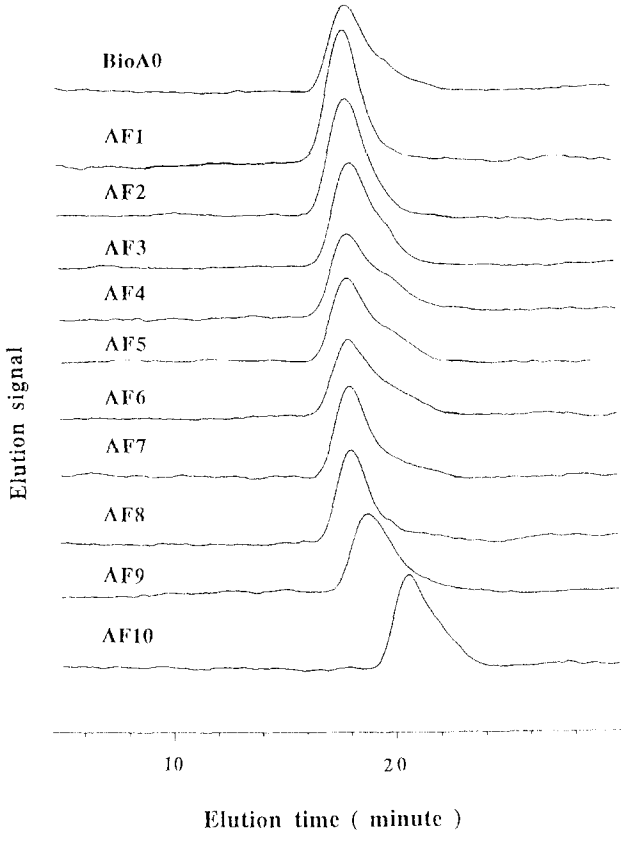

Figure 5 The g.p.c. elution curves for BioA0 and the fractionated copolyesters (AF1–AF10)

Table 3 The characteristics of fractions originated from BioA0 with 36.5 mol.% 3HP unit

Sample code	Heptane (vol.%)	Weight (%)[a]	3HP[b] (mol.%)	M_n[c] ($\times 10^{-5}$)	PDI (M_w/M_n)	Carbonyl diad relative intensity[d]				
						3HP-3HP	3HP-3HB	3HB-3HP	3HB-3HB	D^e
A0	—	100	36.5	2.65	2.53	0.21(0.13)	0.16(0.23)	0.18(0.23)	0.45 (0.40)	3.28
AF1	38.0	4.9	73.6	4.49	1.76	0.44(0.54)	0.21(0.19)	0.24(0.19)	0.11(0.07)	0.96
AF2	39.5	9.0	60.1	3.33	2.12	0.35(0.36)	0.25(0.24)	0.24(0.24)	0.16(0.16)	0.93
AF3	41.0	12.5	53.1	3.09	1.90	0.32(0.28)	0.26(0.25)	0.24(0.25)	0.18(0.22)	0.92
AF4	42.5	11.4	48.0	1.65	3.43	0.23(0.23)	0.24(0.25)	0.24(0.25)	0.29(0.27)	1.16
AF5	44.0	9.9	38.3	2.17	2.97	0.18(0.15)	0.20(0.24)	0.23(0.24)	0.39(0.38)	1.53
AF6	45.5	22.1	21.9	2.03	2.90	0.06(0.05)	0.15(0.17)	0.14(0.17)	0.65(0.61)	1.86
AF7	47.0	12.3	23.8	2.40	2.51	0.05(0.06)	0.16(0.18)	0.19(0.18)	0.61(0.58)	1.00
AF8	48.5	11.7	15.9	2.57	2.34	0.03(0.03)	0.14(0.13)	0.13(0.13)	0.70(0.71)	1.15
AF9	50.0	5.7	13.2	1.79	1.86	0.02(0.02)	0.13(0.11)	0.10(0.11)	0.75(0.75)	1.15
AF10	53.0	0.5	21.6	0.50	1.58			n.a.		

[a]Weight percentage of each fraction was approximately estimated via the weight of each fraction divided by the total yield
[b]3HP mol.% were determined by ^{1}H n.m.r. in the solution state
[c]M_n and PDI were measured via g.p.c. (elution rate, 1 ml/min; sample concentration, 1 mg/ml)
[d]Carbonyl diad relative intensities were determined via ^{13}C n.m.r. in the solution state, the data in brackets were theoretically estimated through the random statistical model; n.a., not available due to trace amount of sample.
[e]$D = F_{BB} \cdot F_{PP}/(F_{BP} \cdot F_{PB})$, where F_{BB}, F_{PP}, F_{BP} and F_{PB} represent relative diad intensities, respectively

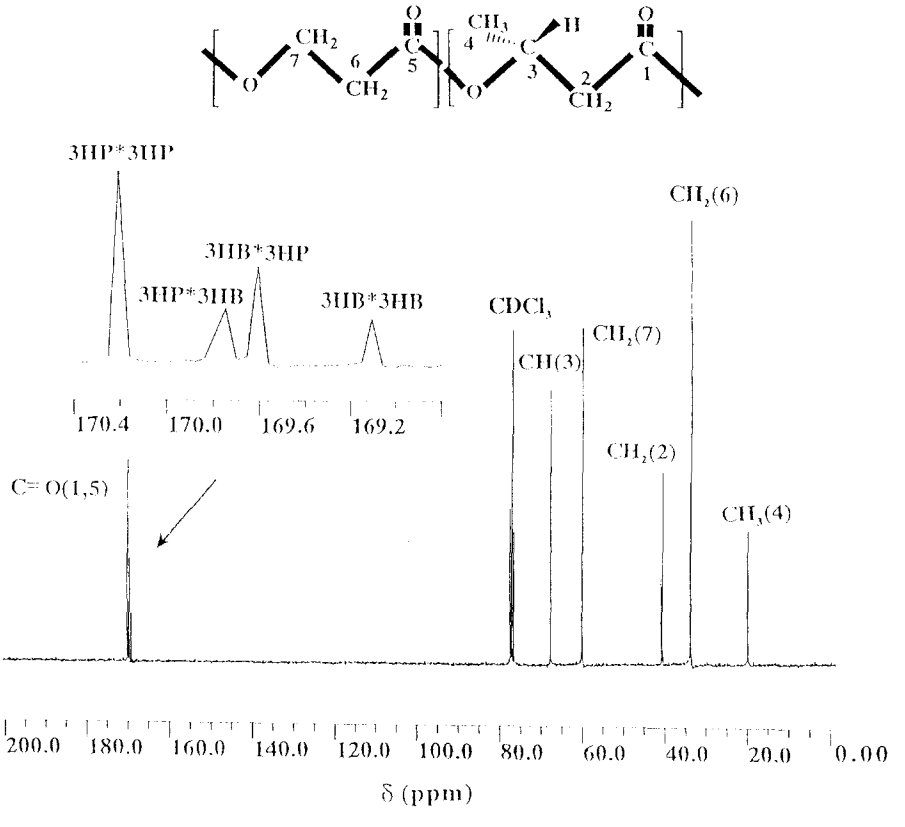

Figure 6 The 67.8 MHz ^{13}C n.m.r. spectrum of the fractionated P(3HB-co-3HP) (fraction AF1) with 73.6 mol.% 3HP unit in $CDCl_3$ solution

Figure 4 for both 'original' BioA0 and BioB0, exhibiting the data for all fractions approximately locate on a straight line despite the origin of either BioA0 or BioB0. Furthermore, G.p.c. results of BioA0 (36.5 mol.% 3HP) and fractions (AF1–AF10) are described in *Figure 5* and also in *Table 3*, in which the elution curves for BioA0 and AF1–AF8 are apparently quite similar. The shift of elution times found for AF9 and AF10 fractions to longer times confirms the appreciable decrease in molecular weight; however, the total percentage of AF9 and AF10 is below 7 wt.%, proving minor components. A similar behavior can also be observed for the BF11 and BF12 fractions. Therefore, it can be concluded that the biosynthesized copolyester P(3HB-co-3HP)s have broad comonomer compositional distributions, and the fractionating behavior as described in this experiment mainly depends on the comonomer composition, while the effects of molecular weight and molecular weight distribution are not so significant[22].

^{13}C solution n.m.r. is an effective tool to analyze the diad sequence distribution for the investigated copolymers[16,22]. *Figure 6* shows the ^{13}C solution n.m.r. spectra of AF1

(73.6 mol.% 3HP), in which the amplified region of carbonyl resonance around 170.0 ppm is also presented. The diads of 3HB*3HB(B*B), 3HB*3HP(B*P), 3HP*3HB(P*B) and 3HP*3HP(P̄*P) were assigned according to the result of Hiramatsu and Doi[10], and their relative intensities were calculated and also listed in *Table 3* for BioA0 along with fractions (AF1–AF9). The values shown in parentheses were estimated based on the random copolymerization model or a Bernoullian model, i.e., each diad relative intensity F_{ij} was estimated from $F_i \times F_j$, where F_i and F_j represent the individual compositions of monomer i and j. In contrast to the results of fractions, the relative diad intensities of 'original' copolyester (BioA0) are considerably deviated from the theoretical values estimated on the Bernoullian model, while experimental values of fractions are obviously in accordance with the theoretical values. A universal parameter expressed as $D = F_{ij}F_{jj}/F_{ij}F_{ji}$ was applied firstly by Inoue and co-workers[22,31] and then by Mitomo *et al.*[21] and Shi *et al.*[16] to characterize the features of diad sequence distribution for copolyesters P(3HB-co-3HV) and P(3HB-co-4HB). Theoretically, the D value is greater than 1.0 for a block-copolymer, while in the case of an alternative copolymer it will be less than 1.0, and will approach 1.0 for a random copolymer. Here, the effect of comonomer compositional distribution on the D parameter is investigated. For this purpose, the D values are hereby simulated on the supposed comonomer compositional distribution function $f(x)$. For the sake of simplicity, a distribution of Gaussian shape ($f(x) = A \exp[-\alpha(x - x_0)^2]$) is adopted on the evidence that the comonomer compositional distribution for either BioA0 or BioB0 is broad and continuous, in which x_0 is the 3HP content at the distribution center, x is the 3HP content of an arbitrarily given component, A and α are the factors defining distribution shape. Further, the comonomer distribution on each constituent copolymer chain is assumed to be statistically random. Varying α in function $f(x)$, the feature of comonomer compositional distribution will be simultaneously changed as exhibited in *Table 4*. Indeed, the dependence of simulated D on the feature of comonomer compositional distribution is obviously indicated, i.e., a broad comonomer compositional distribution will cause an appreciable increase in the D value. Particularly in the case of comonomer compositional distribution with multiple distribution centers (x_{01},x_{02}...) the D values had been reported to increase with the broadness of comonomer composition distribution in a more significant fashion[22]. In *Table 3*, the D values for BioA0 (36.5 mol.% 3HP) as well as the fractions (AF1–AF9) are presented. As compared to the D value of BioA0 ($D = 3.28$), relatively lower D values for fractions are observed, and a tendency of the D values for fractions approaching 1.0 is also indicated. For fractions AF5 and AF6, the fact that the experimental D values are greater than those of other fractions likely stems from the defect caused by the inter-chain entanglement occurring in the fractionating process as discussed above, consequently broadening the comonomer compositional distribution. However, these D values are in fact considerably lower than that of 'original' copolyester BioA0. Comparing the results of experiment and simulation, it can be concluded that copolyester P(3HB-co-3HP)s accumulated as the cell body inclusions virtually obey the random copolymerization model, and this feature is often obscured by the presence of comonomer compositional distribution.

Table 4 The estimation of diad distribution on the supposed mathematical distribution model $f(x) = A \exp[-\alpha(x - x_0)^2]$

Half-height width (ν in mol.%)	$D = F_{BB}{\cdot}F_{PP}/(F_{BP}{\cdot}F_{PB})$			
	α	$x_0 = 36$	$x_0 = 45$	$x_0 = 50$
1	27725.8	1.00	1.00	1.00
5	1109.00	1.01	1.01	1.01
10	277.26	1.02	1.02	1.02
15	123.23	1.05	1.04	1.04
20	69.31	1.09	1.07	1.07
25	44.36	1.13	1.12	1.11
30	30.81	1.19	1.17	1.16
35	22.63	1.25	1.23	1.22
40	17.33	1.33	1.29	1.29
50	11.09	1.44	1.40	1.40

Note: x_0, the assumed 3HP unit content of component copolyester at the comonomer compositional distribution center; x, the 3HP unit content of a given component copolyester; α, the factor regulating the curve shape of comonomer compositional distribution; $\Delta x_i = 1.0/N$ expresses the integral step ($N = 100\,000$); $F_{PP} = \Sigma x^2 f(x)\Delta x_i/\Sigma f(x)\Delta x_i$ ($i = 1, N$); $F_{PB} = \Sigma x(1 - x)f(x)\Delta x_i/\Sigma f(x)\Delta x_i$ ($i = 1, N$); $F_{BP} = \Sigma(1 - x)xf(x)\Delta x_i/\Sigma f(x)\Delta x_i$ ($i = 1, N$); $F_{BB} = \Sigma(1 - x)^2 f(x)\Delta x_i/\Sigma f(x)\Delta x_i$ ($i = 1, N$)

X-ray diffraction and crystal structure

Recently, the effect of solid structures such as the crystal structure, degree of crystallinity, average lamellar size, and so forth on both the environmental and enzymatic biodegrading features has been extensively investigated for either bacterial or synthetic PHAs by Koyama and Doi[32,33] and Kasuya *et al.*[34]. The fact that hydrolysis efficiencies were lowered with the increasing crystallinity and average lamellar size was therein clearly indicated, i.e., the morphological features will play an important role on the apparent biodegradable behaviors. Hence, the crystal structures of the fractionated copolyesters were analyzed along with the 'original' bacterial products.

Figure 7 shows the photographs of X-ray diffraction for homopolymer P(3HB), P(3HP) along with the fractionated P(3HB-co-3HP) samples. On observation, these diffraction patterns can be obviously divided into two distinctive groups (upper and below photographs in *Figure 7*). The diffraction rings which correspond to different d-spacing values of crystallographic planes reflect the essential crystal structure for the investigated semi-crystalline polymers. Okamura and Marchessault[35] have reported that P(3HB) formed an orthorhombic and compact left-handed helix structure (space group $P2_12_12_1$, $a = 0.576$ nm, $b = 1.320$ nm, c(fiber period) $= 0.596$ nm). The crystal structures of bacterial P(3HB-co-3HP)s (original products) with lower 3HP moiety content (0–43 mol.%) have already been investigated by Shimamura *et al.*[11] and Ichikawa *et al.*[12], indicating the presence of only the P(3HB) type of lattice structure. Inspecting the X-ray diffraction patterns presented in *Figure 7*, it is seen that AF9 (13.2 mol.% 3HP) and AF7 (23.8 mol.% 3HP) formed the same crystal structure as P(3HB) (upper half). On the other hand, to our knowledge, the crystal structures for P(3HB-co-3HP)s having higher 3HP mole fractions still remain unknown. In this study, the desired samples with higher 3HP unit monomer fractions (60–96 mol.% 3HP) were successfully prepared with the aid of fractionation, and X-ray diffraction patterns are simultaneously depicted in *Figure 7* (lower half). Interestingly, in contrast to the patterns for P(3HB), AF9 and AF7 (upper), the features of diffraction rings for P(3HP), BF1 (95.9 mol.% 3HP) and BF2 (89.6 mol.% 3HP) (below) are clearly different. However, P(3HP), BF1 and

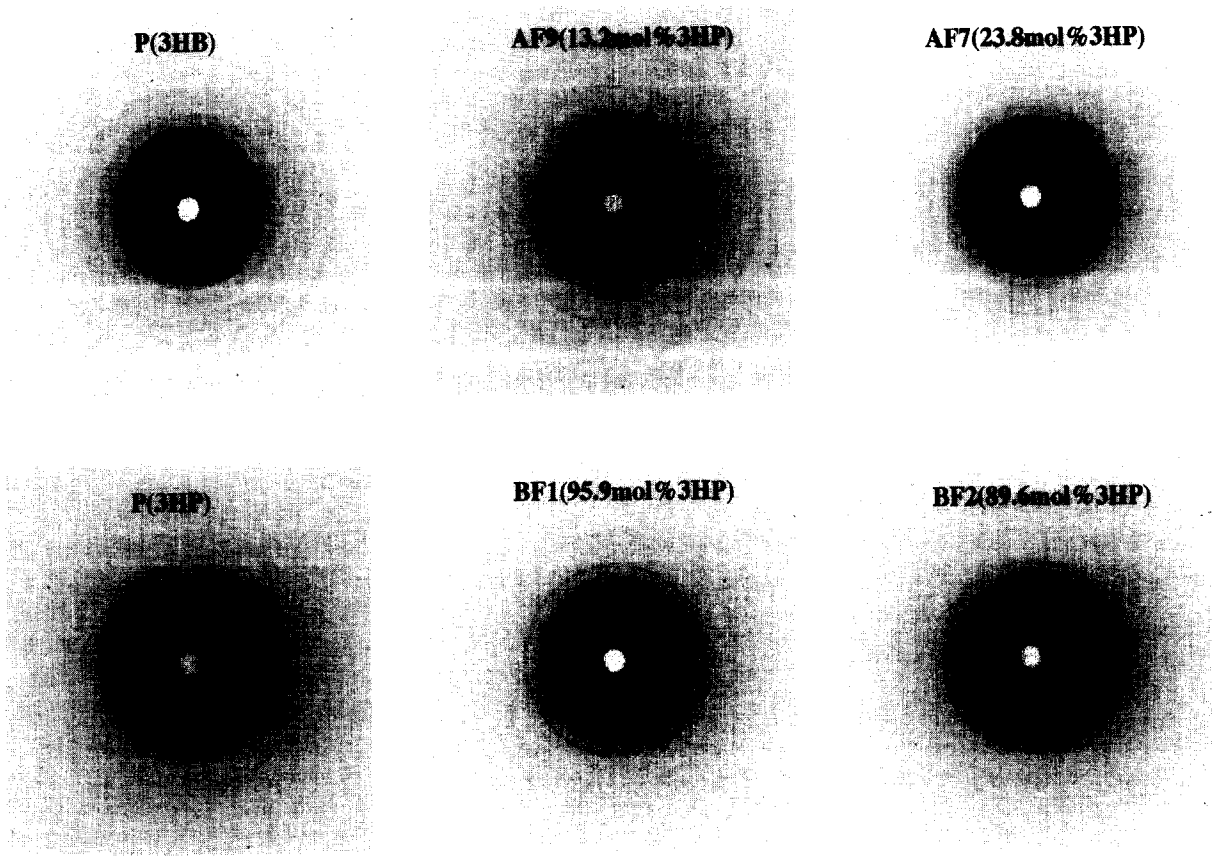

Figure 7 The wide-angle X-ray diffraction patterns for the fractionated copolyesters along with homopolymers P(3HB) and P(3HP)

Table 5 Crystallographic parameters and degrees of crystallinity of the fractionated P(3HB-co-3HP)s estimated from wide-angle X-ray diffraction pattern

Sample code	3HP (mol.%)	Crystallographic parameters			Crystallinity (%)[a]
		a (nm)	*b* (nm)	*c* (nm)	
P(3HB)[b]	0	0.572	1.32	0.595	62.1
BioA0	36.5	0.570	1.32	0.599	30.2
AF9	13.2	0.570	1.31	0.599	50.9
AF8	15.9	0.570	1.31	0.597	48.3
AF7	23.8	0.569	1.31	0.598	39.1
AF6	21.9	0.570	1.31	0.599	40.1
AF5	38.3	0.569	1.31	0.598	16.1
AF2	60.1		n.d[c]		0
BioB0	68.1				18.5
BF4	77.9				20.6
BF3	86.2				23.1
BF2	89.6				44.0
BF1	95.9				57.6
P(3HP)[d]	100				61.7

[a]Calculated according to Vonk's method[26].
[b]As-purchased natural polyester which was used after purification with chloroform and hexane
[c]Not detected
[d]Chemically synthesized poly(β-propiolactone)

BF2 explicitly share the same features of diffraction except for X-ray diffraction intensities, implying that they have the same crystal structure. Suehiro *et al.*[30] and Wasai *et al.*[36] have revealed that there are two modifications of crystal structure for poly(β-propiolactone) [P(3HP)] defined as α and β forms, respectively, representing the 2_1 helix (fiber repeat 0.702 nm) and planar-zigzag (fiber repeat 0.482 nm) packing structures. The α-form structure, the more stable energy state, can be prepared via slowly evaporating chloroform during the casting procedure. The present criterion that fiber period is equal to 0.701 nm (2θ = 25.4°) confirms that P(3HP) and P(3HB-co-3HP)s with higher 3HP contents organized α-form (helix)crystalline structure.

Furthermore, the plots of diffraction intensity *versus* 2θ degrees are also presented in *Figures 8 and 9* for P(3HB),

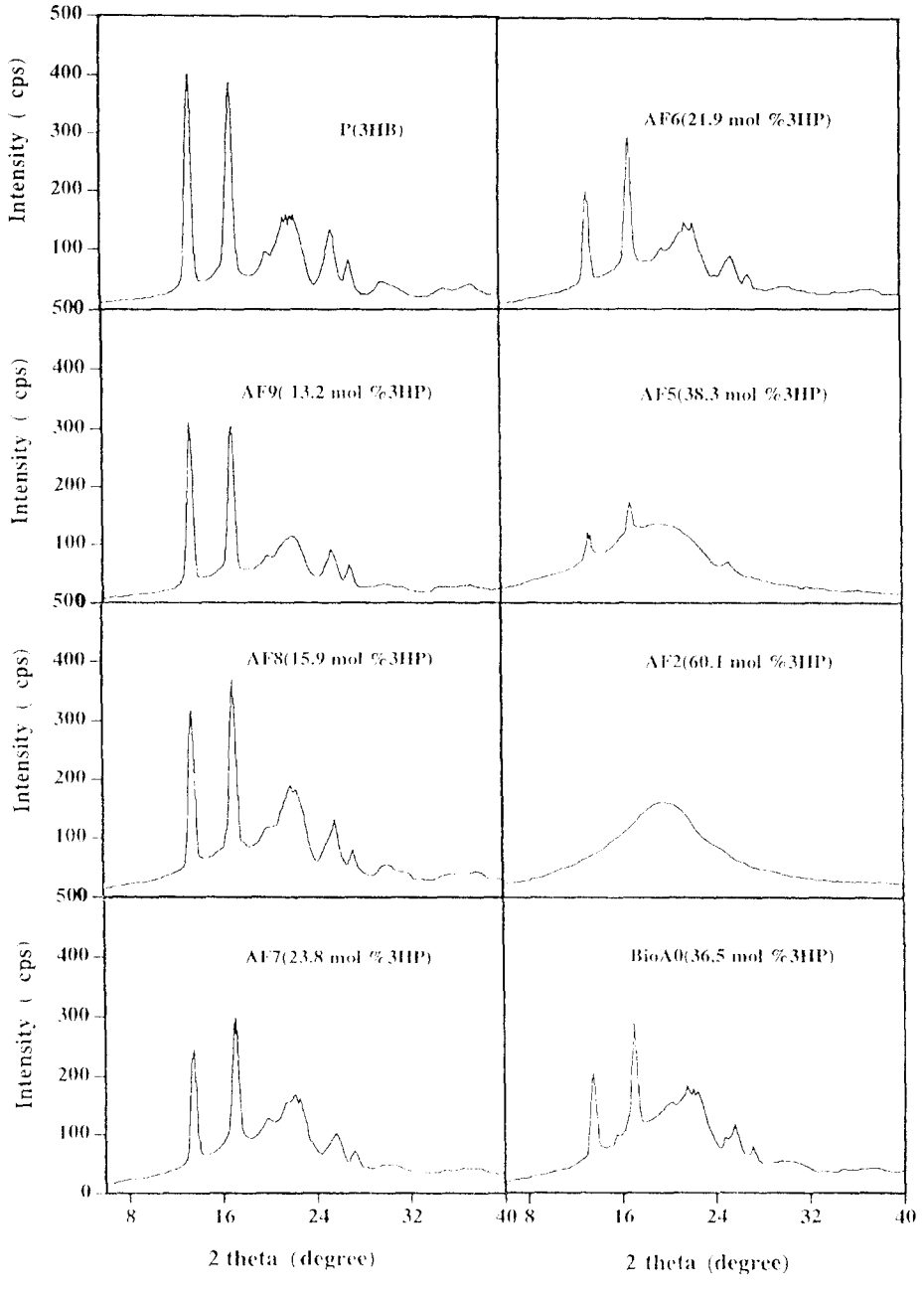

Figure 8 Diffraction intensities *versus* 2θ degrees for P(3HB) BioA0 (36.5 mol.% 3HP) and fractions from BioA0

P(3HP) BioA0, BioB0 along with the fractionated samples with 3HP mol.% spanning the entire comonomer composition range (0–100 mol.%). Inspecting the results illustrated in *Figure 8*, the 2θ degrees corresponding to *d*-spacing values approximately remain constant despite the variation in 3HP mole fraction (13.2–38.3 mol.%) for the fractionated samples, and AF2 (60.1 mol.% 3HP) shows an uncrystalline behavior. The crystallographic parameters of fractions (AF9–AF5) as well as P(3HB) are calculated and listed in *Table 5*, and the deviation in crystallographic parameters observed for copolyesters can be rationalized by the structure distortion caused by the presence of incorporated second comonomer. The degrees of crystallinity (χ_c) estimated in accordance to the Vonk's method obviously decrease with an increase of 3HP fractions of the fractionated copolyesters. On the other hand, for the fractions with higher 3HP mole content (BF1(95.9 mol.% 3HP)–BF4(77.9 mol.% 3HP)), *d*-spacing values remain unchanged regardless of difference in the 3HP monomer fraction, e.g., the 2θ values around 25.4° corresponding to d_{002} are constant[33], the same position of 2θ as that for P(3HP) is explicitly observed. Moreover, the degrees of crystallinity markedly decrease in the order of BF1, BF2, BF3 and BF4, a manner of decreasing 3HP monomer fraction. Viewing the results of BioA0 and BioB0, the unexpectedly higher degree of crystallinity can be reasonably interpreted by the existence of broad comonomer composition distribution, i.e., for the unfractionated samples, the contributions stemming from crystallizable components of increased population lead to the increase in the overall degrees of crystallinity. Based on the evidences of WAXD, it is seen that incorporating a second comonomer into chains of either P(3HB) or P(3HP) will cause the marked suppressing effect on the crystallization driving force, consequently retards the crystallizability of resultant copolyester P(3HB-co-3HP),

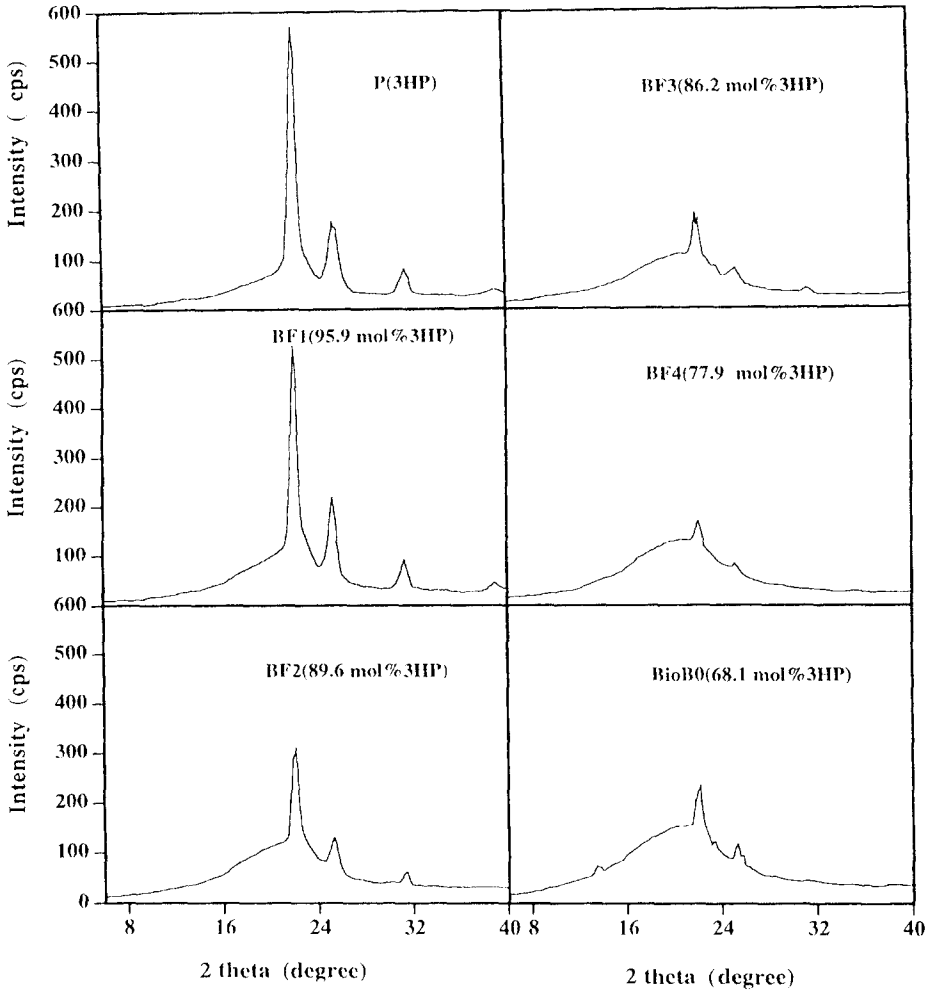

Figure 9 Diffraction intensities *versus* 2θ degrees for P(3HP), BioB0 (68.1 mol.% 3HP) and fractions from BioB0

and that 3HB-rich (0–38.3 mol.% 3HP) and 3HP-rich (77.9–100 mol.% 3HP) copolyesters form distinct helix structures, while copolyesters with 3HP monomer fraction ranging from about 45 to 75 mol.% appear as the amorphous state.

Thermal and crystallization behaviors of the fractionated P(3HB-co-3HP)s

Thermal and crystallization behaviors were also characterized for the fractionated copolyester P(3HB-co-3HP)s. In this study, thermal histories arising from the solvent-casting procedure have already been removed prior to analysis, and thermal diagrams are shown in *Figures 10 and 11* for the fractions along with the 'original' BioA0 and BioB0. Inspecting *Figure 10*, a broader temperature range of melting (about 100–170°C) is observed for the unfractionated BioA0 (36.5 mol.% 3HP) (upper); comparatively, the fractions (AF9–AF7) exhibit the narrower temperature ranges of melting processes. Based on these facts, it can be suggested that the 'original' bacterial copolyester is a mixture composed of a large number of components with different melting points (T_m). The endothermic curves of fractions (AF1–AF4) with 3HP unit content ranging from about 48 to 74 mol.% apparently appear as straight lines, indicating that they are in the amorphous states as found by WAXD. Moreover, it is noticeable that two melting peaks locating at 164.9 and 58.9°C are detected for AF5, and similar behaviors were also reported in our previous work[12]. As compared to the

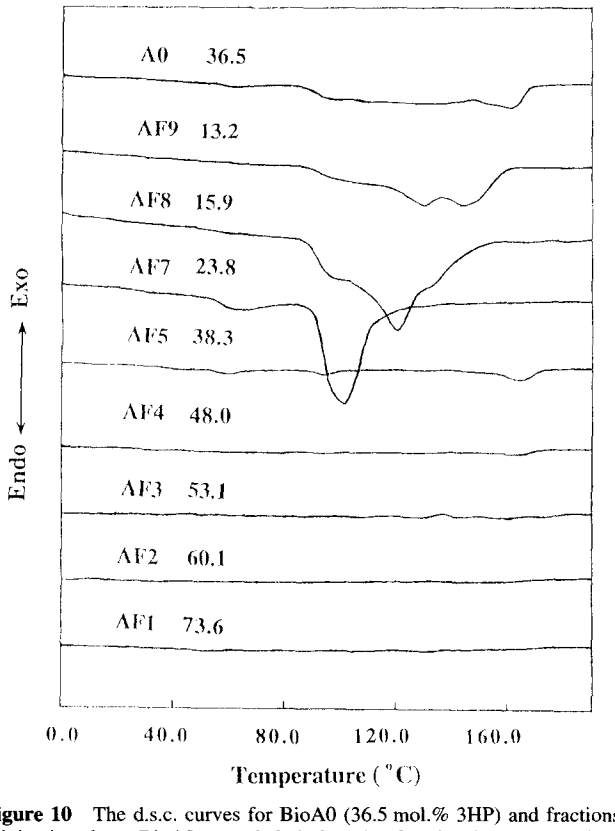

Figure 10 The d.s.c. curves for BioA0 (36.5 mol.% 3HP) and fractions originating from BioA0 recorded during the first heating scan (values following the codes of samples express their corresponding 3HP comonomer compositions)

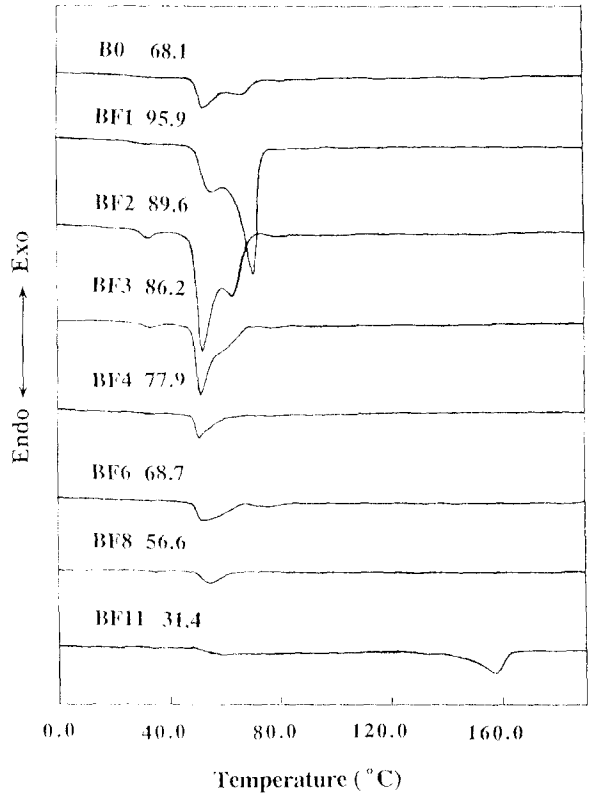

Figure 11 The d.s.c. curves for BioB0 (68.1 mol.% 3HP) and fractions originating from BioB0 recorded during the first heating scan (values following the codes of samples express their corresponding 3HP comonomer compositions)

other fractions, a higher value of parameter D ($D = 1.53$) has been evaluated for AF5 in the former part, indirectly revealing a relatively broader comonomer compositional distribution. Hence, if the comonomer compositional distribution of an investigated copolyester P(3HB-co-3HP) spans two separated crystallizable regions (regions of P(3HB) type lattice and P(3HP) type lattice), two kinds of crystals will be simultaneously presented, leading to the emergence of two separated melting peaks in the endothermic curve. In *Figure 11*, the fractionated samples (BF6–BF8) with the 3HP unit content locating in the region of 48–74 mol.% do not appear as the expected amorphous states, which is not well in agreement with the result for the fractions originated from BioA0. This contradiction may stem from their different features of comonomer compositional distribution. Melting points (T_m) and heat of fusion (ΔH) are estimated from the endothermic curves (first heating scan), and hereby summarized in *Table 6*. On the whole, for the fractionated copolyester P(3HB-co-3HP)s, a trend is clearly indicated, i.e., melting point (T_m) and heat of fusion (ΔH) firstly decrease with the increase in the 3HP monomer fraction (0–40 mol.% 3HP), then they cannot be detected (AF1–AF4 48–75 mol.% 3HP), implying the amorphous aggregating state, finally increase with further increase in 3HP monomer content (75–100 mol.% 3HP). The results of thermal analysis are well consistent with the facts provided by X-ray diffraction discussed above.

Glass transition temperature (T_g) is a conventional criterion to assess segmental mobility for an given polymer or miscibility for an investigated polymer blend in the amorphous state[37]. After rapidly quenching from the melts of original copolyesters and fractions, glass transition behaviors were characterized as depicted in *Figures 12 and 13*. As listed in *Table 6*, the higher 3HP monomer fraction copolyester chains have, the lower glass transition temperatures are detected. Comparing the repeating units of 3HB and 3HP, the methyl group at the β site for the 3HB unit is substituted by a proton for the 3HP unit; consequently the segmental mobility of the 3HP unit is raised owing to the less steric hindrance. The carbon spin-lattice relaxation behavior of P(3HB-co-3HP)s with 0–37 mol.% 3HP content studied by high-resolution solid ^{13}C n.m.r. revealed that the

Table 6 Thermal characteristics of the fractions originated from natural copolyesters BioA0 and BioB0

Sample code	3HP (mol.%)[a]	T_m (°C)[b]	ΔH (J g^{-1})[b]	T_g (°C)[c]
BioA0	36.5	160.6 (61.3)[d]	28.43 (0.91)[d]	−2.4
AF1	73.6	n.d[e]	n.d	−9.6
AF2	60.1	n.d	n.d	−8.1
AF3	53.1	n.d	n.d	−7.4
AF4	48.0	164.4	2.19	−5.8
AF5	38.3	164.9 (58.9)	8.33 (0.82)	−4.0
AF7	23.8	101.6	41.92	−0.8
AF8	15.9	120.6	62.87	1.7
AF9	13.2	130.4	66.47	2.1
BioB0	68.1	52.9	17.94	−12.1
BF1	95.9	70.9	68.45	−17.9
BF2	89.6	63.3	39.08	−14.8
BF3	86.2	51.5	23.21	−13.8
BF4	77.9	51.0	14.87	−12.6
BF6	68.7	52.3	7.14	−10.5
BF7	65.0	56.8	7.69	−10.0
BF8	56.6	55.1	3.40	−8.5
BF10	48.9	160.3 (54.3)	6.68 (3.93)	−4.8
BF11	31.4	157.4	21.81	−3.8

[a]Determined by ^1H n.m.r. ($CDCl_3$) in the solution state
[b]T_m and ΔH of samples prepared via cooling from the melt were estimated by d.s.c. in the first heating scan with heating rate 10°C/min
[c]Measured by d.s.c. in the second heating scan with heating rate 20°C/min
[d]Data in the parentheses corresponding to the minor melting peak
[e]Not detected

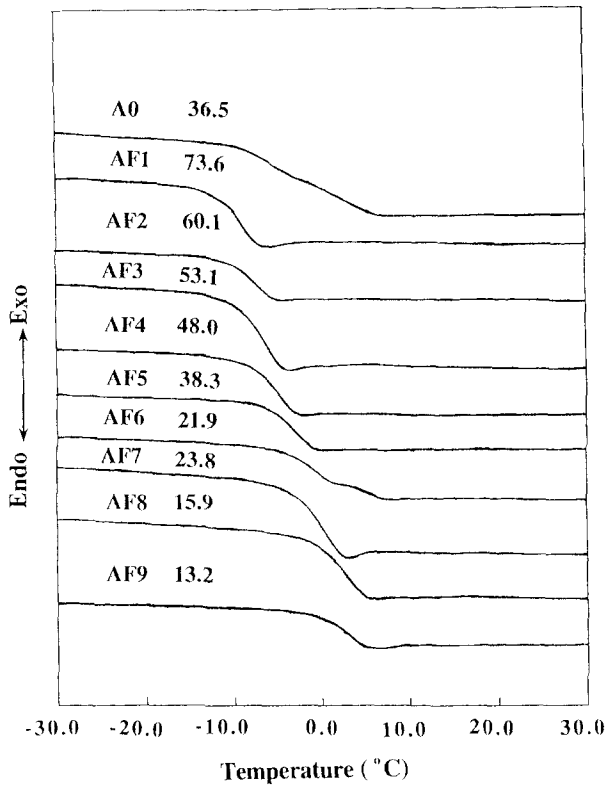

Figure 12 The d.s.c. curves for BioA0 (36.5 mol.% 3HP) and fractions originating from BioA0 recorded during the second heating scan (values following the codes of samples express their corresponding 3HP comonomer compositions)

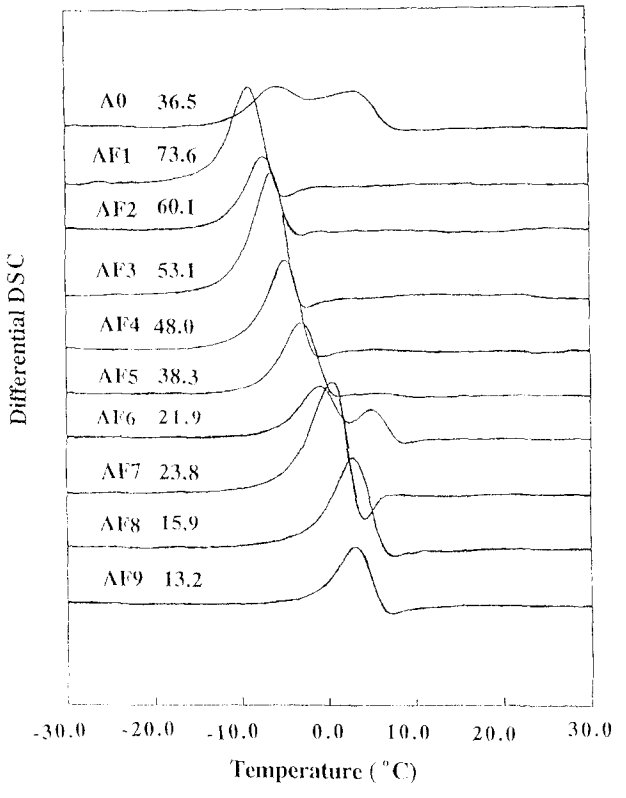

Figure 14 The differential d.s.c. curves for BioA0 (36.5 mol.% 3HP) and fractions originating from BioA0 recorded during the second heating scan (values following the codes of samples express their corresponding 3HP comonomer compositions)

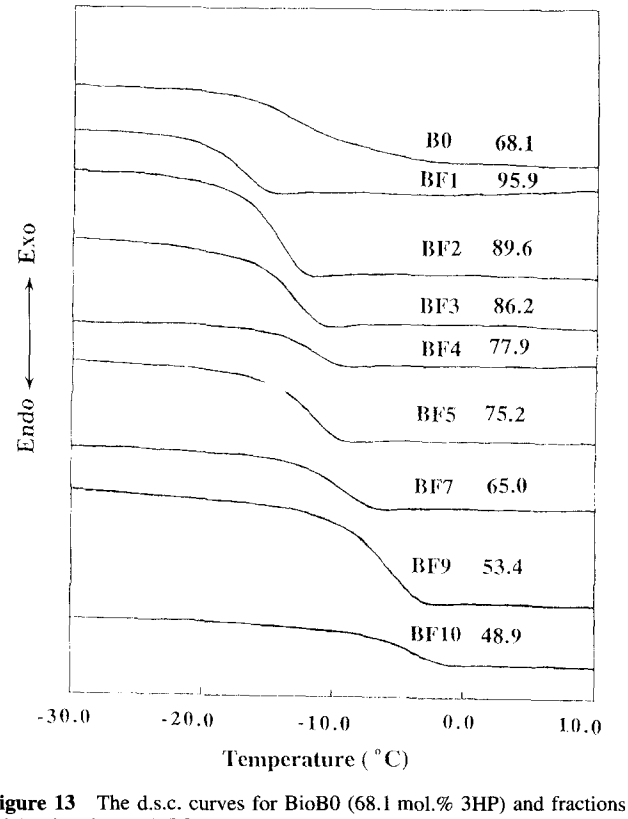

Figure 13 The d.s.c. curves for BioB0 (68.1 mol.% 3HP) and fractions originating from BioB0 recorded during the second heating scan (values following the codes of samples express their corresponding 3HP comonomer compositions)

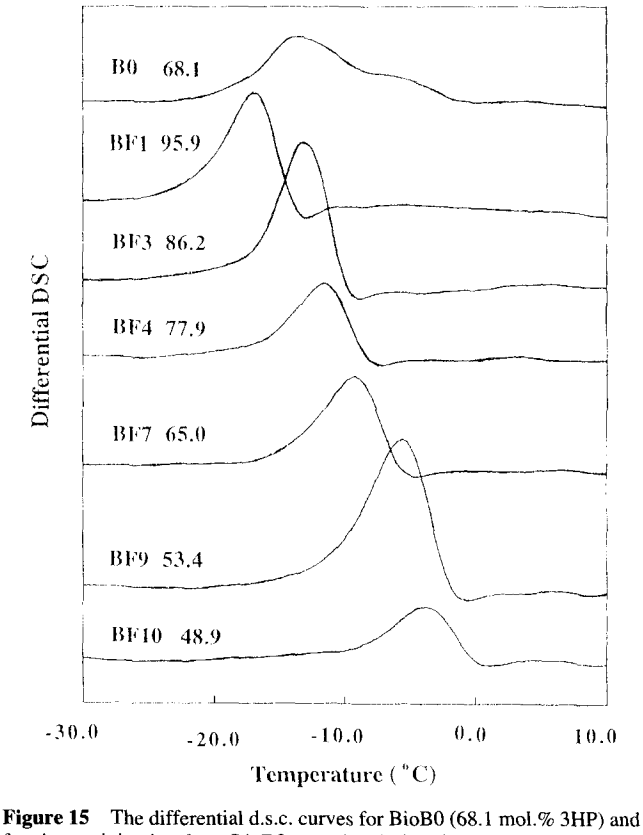

Figure 15 The differential d.s.c. curves for BioB0 (68.1 mol.% 3HP) and fractions originating from BioB0 recorded during the second heating scan (values following the codes of samples express their corresponding 3HP comonomer compositions)

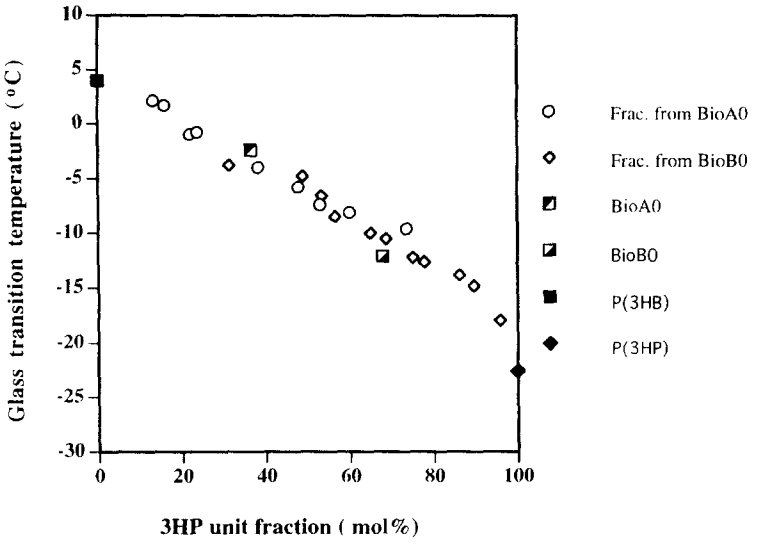

Figure 16 The dependence of glass transition temperature (T_g) on the 3HP unit contents for the fractionated copolyesters as well as the original BioA0 and BioB0

mobility of 3HB units in the amorphous region increases with the content of the 3HP unit[12]. Recently similar behaviors have been observed for P(3HB-co-4HB)[15], indicating that the monomer units with less steric hindrance, such as the 3HP and the 4HB, enhanced the segmental mobility in the amorphous region of copolymers.

On the other hand, it is noticeable that the glass transition features in detail of original and fractionated copolyesters are quite different, i.e., broader temperature ranges of glass transition are observed for original products BioA0 and BioB0. To clarify the behaviors of glass transition, differential d.s.c. diagrams for BioA0, BioB0 and fractions were also measured and are shown in *Figures 14 and 15*. Interestingly, multiple peaks of heat capacity change are obviously exhibited for BioA0, BioB0 and AF6, while the other fractions show single transition peaks. In particular, for BioA0, two peaks are well separated, evidently indicating original BioA0 is a mixture of components which are immiscible with each other in the molten state. The d.s.c. peaks locating at the higher and lower temperatures, respectively, correspond to the glass transitions of copolyester chains with lower and higher 3HP monomer fractions in the original product. Result of AF6 shows the similar behavior as the original products BioA0 and BioB0, revealing the defect of fractionation as discussed on the value of D parameter. Based on this evidence, it is demonstrated that the result of glass transition can provide us an indirect way to assess comonomer compositional distribution of investigated copolyester P(3HB-co-3HP)s. The difference of 3HP monomer fractions in copolyester chains to a certain extent indeed causes the transition of melt of copolyesters from miscible to immiscible. However, the exact difference of 3HP monomer fraction at the transition point is still unknown. In general, it will be regulated by the average comonomer composition and comonomer compositional distribution. *Figure 16* describes the relationship between glass transition temperature (T_g) and 3HP unit mole fraction of copolyester. Within the whole comonomer composition range, a good linearity is exhibited, indicating that the segmental mobilities of copolyester chains are proportional to their 3HP comonomer compositions[13].

Spherulitic growth rates G have been also measured for the fractionated P(3HB-co-3HP)s, and the growth rates

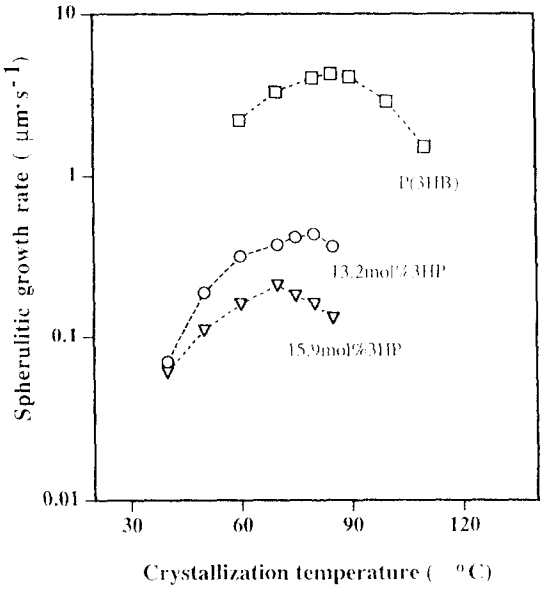

Figure 17 The spherulitic growth rates of P(3HB) and the fractionated copolyesters (AF8–AF9) at the various isothermal crystallization temperature (T_c)

estimated as the slope of dR/dt are depicted in *Figure 17*. It is seen that spherulitic growth rates are drastically suppressed by about one order of magnitude when the 3HP comonomer fraction increases from 0 (P(3HB)) to 15.9 mol.% (AF8). T_{cmax} denoted as the isothermal crystallization temperature (T_c) at which the maximum growth rate is observed, is about 85°C for P(3HB) which is similar to the data as reported[11–13], while those of the fractionated samples AF9 and AF8 are about 80 and 70°C, respectively. The T_{cmax} values clearly indicate a tendency to move to lower temperature with increasing the 3HP comonomer composition of the copolyester chains.

Shimamura *et al.*[11] had reported that the G_{max} value (at T_{cmax} = 80°C) was about 0.06 μm s^{-1} for an original unfractionated product P(3HB-co-11.0 mol.% 3HP) which is considerably lower than the value of 0.42 μm s^{-1} for AF9 (13.2 mol.% 3HP) obtained in this work. On the other hand, a higher G_{max} value for unfractionated P(3HB-co-13 mol.% 3HP) had also been reported to be about 2.0 μm s^{-1} by

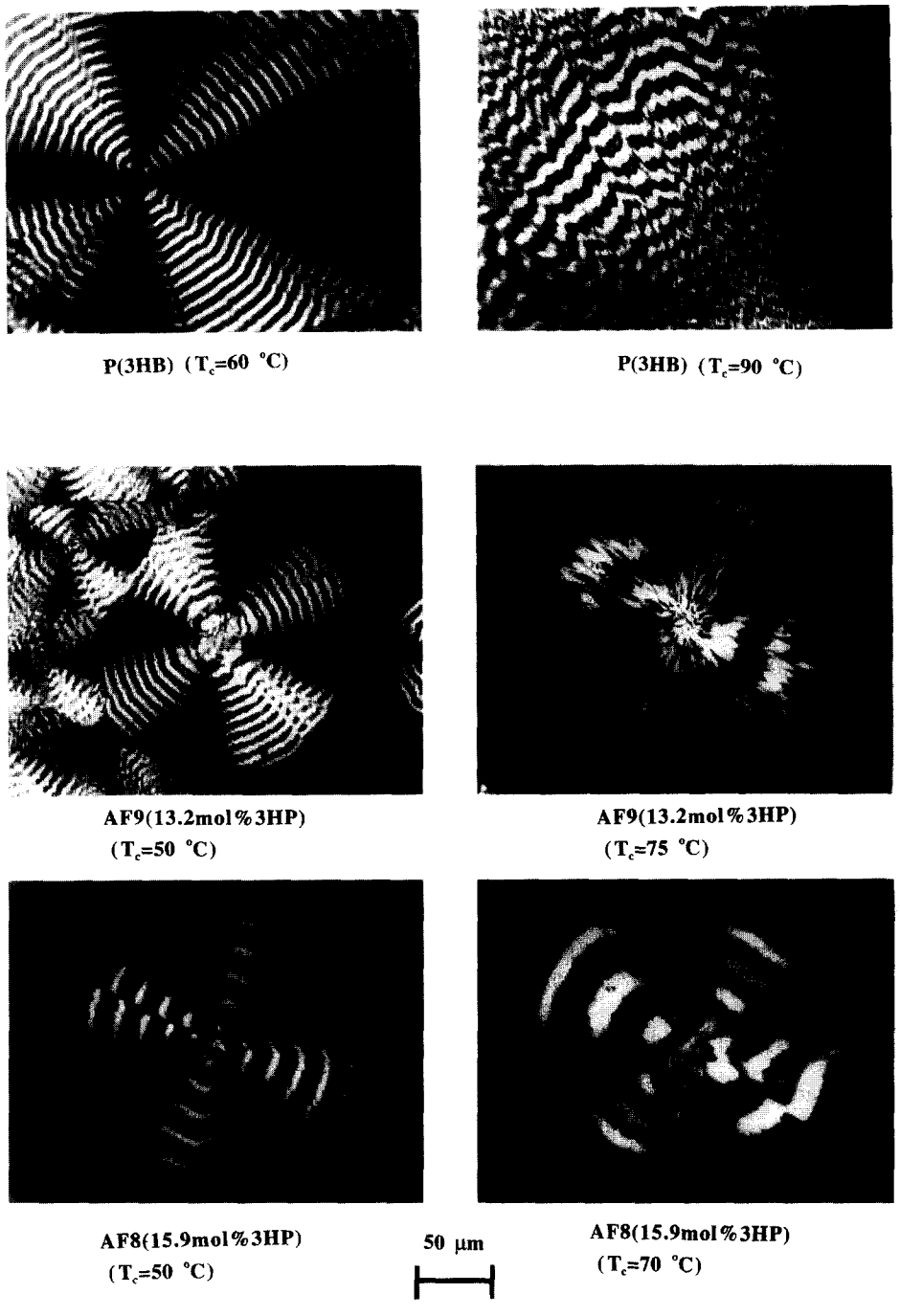

Figure 18 The photographs of spherulites for P(3HB) and the fractionated copolyesters recorded at different isothermal crystallization temperatures

Ichikawa *et al.*[12]. The appreciable difference in the G_{max} values among three individual works likely stems from the distinctive features of comonomer composition distributions for the investigated copolyesters, although they have similar mean 3HP comonomer compositions. If the population of copolyester fractions with lower 3HP comonomer content (having higher melting point and higher crystallization tendency) than the average value of the original product increase, hence, at a given isothermal crystallization temperature (T_c) the degree of supercooling ($\Delta T = T_m - T_c$) is increased for some copolymer fractions, consequently, the driving force of crystallization becomes larger, and a higher growth rate can be observed. Since the individual features of comonomer compositional distribution determine the populations of copolyester chains with various 3HP comonomer contents, therefore, the apparent growth behaviors of spherulite are considerably different for the fractionated and original copolyesters. Viewing these facts, it is necessary to take the factors of comonomer compositional distribution and miscibility among the fractions into consideration for assessing the crystallizability of an investigated copolyester P(3HB-co-3HP). On the other hand, for P(3HP) and the fractionated copolyesters with higher 3HP comonomer contents, the spherulites were found to indeed form; however, it was practically too difficult to measure the growth rate due to the fact that, even at a $\Delta T = T_m - T_c = 5$–8°C, the nucleation densities would be so high that the growing spherulites were quickly impinged, and the ultimate dimensions of spherulites were about ≈ 10 μm (not shown here), indicating the formation of the micro-crystal structures.

Figure 18 shows the representative textures of spherulites for P(3HB) and the copolyester fractions AF9 and AF8. It is obvious that the spherulites formed at lower isothermal

crystallization temperature exhibit the well-known banded structures which have already been interpreted due to the presence of twisted lamella originating from the stress built-up during crystallization[37,38]. Inspecting the photographs of spherulites for P(3HB) and copolyesters, the more coarse textures are obviously seen in the case of either raising the T_c or increasing the 3HP mole fraction of copolyester chains. For copolyester, owing to the existence of comonomer compositional distribution, the chains bearing higher 3HP fractions than the average 3HP comonomer composition to a certain extent will become uncrystallizable under a lower supercooling condition ΔT. The possible places that the uncrystallizable chains can exist are interlamellar, interfibrillar and intrafibrillar regions[37], the morphological evidence of spherulites of AF9 and AF8 suggest that the uncrystallizable chains were likely trapped in the interfibrillar regions.

CONCLUSIONS

In summary, two kinds of copolyesters (BioA0, and BioB0) with respective 3HP comonomer fractions of 36.5 and 68.1 mol.% have been accumulated by the bacteria *A. latus* via varying the feeding weight ratio of carbon substrates ((*R*)-3-hydroxybutyric acid: 3-hydroxypropionic acid 1:5 and 4:2), however, either yield of dry cells or polymer content was drastically decreased with the increasing 3HP comonomer fraction of bacteria product. Through chloroform (solvent)/*n*-heptane (nonsolvent) fractionating technique, the harvested copolyesters were fractionated, unambiguously indicating the broad comonomer compositional distribution features as reported in our previous report[13], i.e., for BioA0, the 3HP comonomer composition of the fractionated samples ranged from 13.2 to 73.6 mol.%, similarly, for BioB0 the comonomer compositional distribution spanned the range of 31.4 to 95.9 mol.%. G.p.c. analysis explicitly revealed that the fractionating procedure was actually governed by the factor of comonomer composition in a more significant fashion than that of molecular weight. ^{13}C solution n.m.r. analysis of carbonyl diad sequence distribution for the original and the fractions indicated that the copolyesters accumulated as cell body inclusions were virtually consistent with the random copolymerization model, and the 'true' features were, however, likely obscured by the presence of comonomer compositional distribution, especially for the original bacterial products. X-ray diffraction patterns exhibited that both 3HB- and 3HP-rich copolyesters indeed organized distinctive crystal structures as P(3HB) and P(3HP) types of lattice, respectively. Interestingly, the 3HP-rich copolyesters adopted the 2_1 helix structure as the more stable energy state than the other possible planar-zigzag packing structure. In thermal analysis, the resulting peak occurring at the higher or lower temperature was found to reflect the above-mentioned crystalline structures. For samples with medium 3HP comonomer contents, only amorphous aggregating states were detected. The glass transition behaviors for the 'original' and fractionated copolyesters indicated that the T_g linearly decreased with the increase in 3HP monomer content, proving the enhanced segmental mobility, and the difference in comonomer composition among the component copolyesters to a certain extent would lead to immiscible property in the molten state. Furthermore, investigating the spherulitic growth and crystal morphology, it was demonstrated that incorporating a minor comonomer would cause a marked suppressing effect on the formation of crystal structure, resulting in an apparent decrease of spherulitic growth rate. The coarse textures of spherulites for copolyesters suggest that the uncrystallizable chains were likely trapped in the interfibrillar regions.

On the basis of this study, the dependence of both environmental and enzymatic degrading features on the comonomer composition, comonomer compositional distribution and morphology can be reasonably expected for bacterial P(3HB-co-3HP)s, and which are now under the investigation in our laboratory.

ACKNOWLEDGEMENTS

The authors are grateful to Prof. Dr. M. Sumita and Dr. S. Asai of Tokyo Institute of Technology for kindly supporting the measurements of WAXD.

REFERENCES

1. Doi, Y., *Microbial Polyester*. VCH Publisher, New York, 1990.
2. Inoue, Y. and Yoshie, N., *Prog. Polym. Sci.,*, 1992, **17**, 571.
3. Hocking, P. J. and Marchessault, R. H., *Biodegradable Polymer*, ed G. J. L. Griffin. Blackie Academic & Professional, London, New York, 1994.
4. Steinbüchel, A. and Valentin, H.F., *FEMS Microbiol. Lett.*, 1995, **128**, 219.
5. Holmes, P. A., Wright, L. F. and Collins, S. H., Eur. Pat. Appl., 0 052 459, 1981; Eur. Pat. Appl., 0 069 497, 1983.
6. Holmes, P.A., *Phys. Technol.*, 1995, **16**, 32.
7. Doi, Y., Tamaki, A., Kunioka, M. and Soga, K., *Appl. Microbiol. Biotechnol.*, 1988, **28**, 330.
8. Doi, Y., Segawa, A., Nagamura, A. and Kunioka, M., *Novel Biodegradable Microbial Polymers*, ed. E. A. Dawes. Kluwer Academic Publishers, Dordrecht, Boston, 1990.
9. Nakamura, S., Kunioka, M. and Doi, Y., *Macromol. Rep.*, 1991, **A28**(Suppl. 1), 15.
10. Hiramatsu, M. and Doi, Y., *Polymer*, 1993, **34**, 4782.
11. Shimamura, E., Scandola, M. and Doi, Y., *Macromolecules*, 1994, **27**, 4429.
12. Ichikawa, M., Nakamura, K., Yoshie, N., Asakawa, N. and Inoue, Y., *Macromol. Chem. Phys.*, 1996, **197**, 2467.
13. Cao, A., Ichikawa, M., Kasuya, K., Yoshie, N., Asakawa, N., Inoue, Y., Doi, Y. and Abe, H., *Polymer J.*, 1996, **28**, 1096.
14. Nakamura, K., Yoshie, N., Sakurai, M. and Inoue, Y., *Polymer*, 1994, **35**, 193.
15. Spyros, A. and Marchessault, R.H., *Macromolecules*, 1995, **28**, 6108.
16. Shi, F., Ashby, R.D. and Gross, R.A., *Macromolecules*, 1997, **30**, 2521.
17. Abe, H., Doi, Y., Aoki, H., Akehata, T., Hori, Y. and Yamaguchi, A., *Macromolecules*, 1995, **28**, 7630.
18. Valentin, H.E., Schönebaum, A. and Steinbüchel, A., *Appl. Microbial Biotechnol.*, 1996, **46**, 261.
19. Yamashita, M., Hattori, N. and Nishida, H., *Polymer Preprints Japan*, 1994, **43**, 3980.
20. Sharma, R. and Kay, A.R., *J. Macromol. Sci.-Rev., Macromol. Chem. Phys.*, 1995, **C35**(2), 327.
21. Mitomo, H., Morishita, N. and Doi, Y., *Macromolecules*, 1993, **26**, 5809.
22. Yoshie, N., Menju, H., Sato, H. and Inoue, Y., *Macromolecules*, 1995, **28**, 6516.
23. Mizuno, A., Abiru, T. and Weigand, F., *Polymer* (in press).
24. Karoglanian, S.A. and Harrison, I.R., *Thermochim. Acta*, 1996, **288**, 239.
25. Hildebrand, J. and Scott, R. L., *Solubility of Nonelectrolytes*. Reinhold Publishing Corporation, New York, 1949.
26. Vonk, C.G., *J. Appl. Cryst.*, 1973, **6**, 148.
27. Small, P.A., *J. Appl. Chem.*, 1953, **3**, 71.
28. Hoy, K.L., *J. Paint Technol.*, 1970, **42**, 76.
29. Burrell, H., *Polymer Handbook*, 2nd edn., ed. J. Brandrup and E. H. Immergut. John Wiey & Sons, New York, London, Sydeny, Toronto, 1975.

30. Suehiro, K., Chatani, Y. and Tadokoro, H., *Polym. J.*, 1975, **7**, 352.
31. Kamiya, N., Yamamoto, Y., Inoue, Y., Chujo, R. and Doi, Y., *Macromolecules*, 1989, **22**, 1676.
32. Koyama, N. and Doi, Y., *Macromolecules*, 1996, **29**, 5843.
33. Koyama, N. and Doi, Y., *Macromolecules*, 1997, **30**, 826.
34. Kasuya, K., Inoue, Y. and Doi, Y., *Int. J. Biol. Macromol.*, 1996, **19**, 35.
35. Okarnura, K. and Marchessault, R. H., *Comformation of Biopolymers*, ed G. N. Ramachandran. Academic Press, London, 1967.
36. Wasai, T., Saegusa, T. and Fukukawa, J., *Kougyou Kagaku Zasshi*, 1964, **67**, 601.
37. Xing, P., Dong, L., An, Y., Feng, Z., Avella, M. and Martsucell, E., *Macromolecules*, 1997, **30**, 2726.
38. Barham, P.J., Keller, A. and Otun, E.L., *J. Mater. Sci.*, 1984, **19**, 2781.